

Cubic-Quintic Duffing Oscillators

Vivien Chua
vivien@math.gatech.edu
College of Engineering
School of Electrical and Computer Engineering
Georgia Institute of Technology, Atlanta, Georgia 30332

December 12, 2003

Abstract

Duffing oscillators comprise one of the canonical examples of Hamilton systems. However, simple generalizations of such oscillators, such as cubic-quintic Duffing oscillators, have not been studied as extensively. The presence of a quintic term makes the cubic-quintic Duffing oscillator more complex and interesting to study. In this work, we extend the techniques used to investigate Duffing oscillators to cubic-quintic Duffing oscillators. We employ perturbative analytical techniques such as the method of averaging and Lindstedt's method to analyze the forced, damped cubic-quintic Duffing oscillator. In particular, we derive approximate periodic solutions and period-amplitude relations. We also illustrate our analytical investigations with extensive numerical simulations of phase portraits and Poincaré maps of the unforced cubic-quintic Duffing oscillator, the forced cubic-quintic Duffing oscillator with a single sinusoidal forcing term, and the forced cubic-quintic Duffing oscillator with two sinusoidal forcing terms. Varying the parameters of these Duffing oscillators produces a variety of interesting dynamics. For example, the periodic behavior characteristic of the unforced cubic-quintic Duffing equation is no longer evident in some cases.

1 Introduction

Many of the most important problems in classical mechanics may be described by Hamiltonian flows.^{2,4,7,8} Examples of Hamiltonian systems include planetary motion, charged particles in magnetic fields, incompressible fluid flows and mean-field descriptions of Bose-Einstein condensates.^{5,6,9}

Hamilton's equations for autonomous dynamical systems are^{2,3}

$$\begin{aligned}q' &= \frac{dH}{dp}, \\p' &= -\frac{dH}{dq},\end{aligned}\tag{1}$$

where $H(q, p)$ is the Hamiltonian, q is the vector of “generalized coordinates,” and p is the vector of “conjugate momenta.” Hamiltonian systems are time-invariant. When the Hamiltonian is regarded as the energy of the system, this property implies conservation of energy.

Duffing oscillators comprise one of the canonical examples of Hamiltonian systems.^{3,7–9} For a particular choice of parameters, the cubic Duffing oscillator is described by the following equations of motion:

$$\begin{aligned}x' &= \frac{dH}{dy} = y, \\y' &= -\frac{dH}{dx} = -x + x^3,\end{aligned}\tag{2}$$

where $H = y^2/2 - x^2/2 + x^4/4$ is the Hamiltonian.

Duffing’s equation is used to model conservative double-well oscillators, which can occur, for example, in magneto-elastic mechanical systems.³ The system in question consists of a beam placed vertically between two magnets with the top end fixed and the bottom end free to swing. With velocity applied to the beam, the beam starts to oscillate between the two magnets. The beam finally comes to rest at a fixed point and remains in equilibrium. When a (nonautonomous) periodic forcing is applied to the system, the beam oscillates between the two magnets. There are no stable fixed points and no stable fixed cycles in the system. The system is modeled by the forced, damped cubic Duffing equation,

$$x'' + \delta x' + \alpha x + \beta x^3 = F \cos(\omega t),\tag{3}$$

where $\delta < 0$ and α and β can be either positive or negative.

The cubic Duffing oscillator describes the motion of a classical particle in a double well potential,^{3,8}

$$V(x) = -\frac{x^2}{2} + \frac{x^4}{4}.\tag{4}$$

The two wells are separated by a local maximum at $x = 0$. With weak periodic forcing, the particle oscillates with small amplitude and stays near one of the potential’s minima. With strong periodic forcing, however, the particle oscillates with large amplitude between the two wells crosses the local maximum during its motion.

The addition of a quintic term to (3) provides a simple generalization of the Duffing oscillator that has not been as extensively studied as the canonical cubic case. For appropriate parameter choices, this describes a classical particle in a triple-well potential rather than the double-well potentials usually considered. The forced cubic-quintic Duffing oscillator exhibits a wide variety of dynamical behavior that is reflected in its equilibrium points, periodic oscillations, and chaotic dynamics.

In this work, we extend the methods applied to investigate cubic Duffing oscillators to forced cubic-quintic Duffing oscillators. We begin in Section 2 by determining the system’s equilibria in the absence of forcing. In the next several sections, we simulate phase portraits and Poincaré sections of the cubic-quintic

Duffing oscillator numerically both with and without forcing. We consider, in turn, the unforced cubic-quintic Duffing oscillator, periodically forced cubic-quintic Duffing oscillators, and multiple-frequency periodically forced cubic-quintic Duffing oscillators. We subsequently employ perturbative techniques such as Lindstedt's method and the method of averaging to study periodic orbits in the general cubic-quintic Duffing oscillator as well as specific cases for the different values of α , β and γ . We illustrate the application of Chirikov's overlap criterion to this system, and finally summarize the results of this work in a concluding section.

2 Equilibrium Points

The unforced, undamped cubic-quintic Duffing oscillator is given by

$$x'' + \alpha x + \beta x^3 + \gamma x^5 = 0. \quad (5)$$

From (5), we obtain the autonomous dynamical system

$$\begin{aligned} y &= x', \\ y' &= -\alpha x - \beta x^3 - \gamma x^5 \end{aligned} \quad (6)$$

With $x'' = 0$, one sees that $y = 0$. The condition $y' = 0$ implies that $x = 0$ or

$$x_{\pm} = \pm \sqrt{\frac{-\beta \pm \sqrt{\beta^2 - 4\gamma\alpha}}{2\gamma}}. \quad (7)$$

There are equilibria at some x_{\pm} provided

$$\begin{aligned} \text{(a)} \quad & \beta^2 \geq 4\gamma\alpha, \\ \text{(b)} \quad & -\beta \pm \sqrt{\beta^2 - 4\gamma\alpha} \geq 0 \end{aligned} \quad (8)$$

The Jacobian of (6) is

$$A = \begin{bmatrix} 0 & 1 \\ -\alpha - 3\beta x^2 - 5\gamma x^4 & 0 \end{bmatrix}. \quad (9)$$

Its eigenvalues satisfy

$$\lambda^2 = -\alpha - 3\beta x_*^2 - 5\gamma x_*^4, \quad (10)$$

where x_* denotes the x -coordinate of an equilibrium point.

The equilibrium points in the unforced, undamped cubic-quintic Duffing oscillator are thus of the form $(0, 0)$ and $(x_{\pm}, 0)$. The latter class of equilibria come in pairs and exist provided the associated value is real. With damping, the dynamical behavior of the unforced cubic-quintic Duffing oscillator changes, as centers become stable spirals.

Table 1) indicates the dynamics for a few choices of α , β , and γ . We also discuss these situations in the text.

Table of Equilibrium Points

α	β	γ	Equilibria
1	1	1	Center at $(0, 0)$
1	1	-1	Center at $(0, 0)$ and Saddles at $(\pm\sqrt{\frac{\sqrt{5}+1}{2}}, 0)$
-1	1	1	Saddle at $(0, 0)$ and Centers at $(\pm\sqrt{\frac{\sqrt{5}-1}{2}}, 0)$
-1	1	-1	Saddle at $(0, 0)$
-1	1	-0.01	Centers at $(0, 0)$, $(\pm\sqrt{\frac{1-\sqrt{0.96}}{0.02}}, 0)$ and Saddle at $(\pm\sqrt{\frac{1-\sqrt{0.96}}{0.02}}, 0)$
1	-1	1	Center at $(0, 0)$
1	-1	0.01	Centers at $(0, 0)$, $(\pm\sqrt{\frac{1+\sqrt{0.96}}{0.02}}, 0)$ and Saddle at $(\pm\sqrt{\frac{1+\sqrt{0.96}}{0.02}}, 0)$
1	-1	-1	Center at $(0, 0)$ and Saddles at $(\pm\sqrt{\frac{1-\sqrt{5}}{2}}, 0)$
-1	-1	1	Saddle at $(0, 0)$ and Centers at $(\pm\sqrt{\frac{1+\sqrt{5}}{2}}, 0)$
-1	-1	-1	Saddle at $(0, 0)$

Table 1: Table of equilibrium points for various values of α , β and γ

When $\alpha = 1$, $\beta = 1$, and $\gamma = 1$, there is a center at $(0, 0)$ with eigenvalues $\lambda = \pm i$. A phase portrait for this situation is shown in Figure 1.

When $\alpha = 1$, $\beta = -1$, and $\gamma = -1$, there are equilibrium points at $(0, 0)$ and $(\pm\sqrt{\frac{1-\sqrt{5}}{2}}, 0)$. At $(0, 0)$, $\lambda = \pm i$, so this point is a center. At $(\pm\sqrt{\frac{1-\sqrt{5}}{2}}, 0)$, $\lambda \approx \pm 1.663$, so these points are saddles. A phase portrait for this situation is shown in Figure 2.

When $\alpha = 1$, $\beta = -1$ and $\gamma = 0.01$, there are equilibrium points at $(0, 0)$, $(\pm\sqrt{\frac{1+\sqrt{0.96}}{0.02}}, 0)$ and $(\pm\sqrt{\frac{1-\sqrt{0.96}}{0.02}}, 0)$. At $(0, 0)$, $\lambda = \pm i$, so this point is a center. At $(\pm\sqrt{\frac{1+\sqrt{0.96}}{0.02}}, 0)$, $\lambda = \pm i$, so these points are centers. At $(\pm\sqrt{\frac{1-\sqrt{0.96}}{0.02}}, 0)$, $\lambda = \pm 1.663$, so these points are saddles. A phase portrait for this situation is shown in Figure 3.

When $\alpha = -1$, $\beta = 1$, and $\gamma = 1$, there are equilibrium points at $(0, 0)$ and $(\pm\sqrt{\frac{\sqrt{5}-1}{2}}, 0)$. At $(0, 0)$, $\lambda = \pm 1$, so this point is a saddle. At $(\pm\sqrt{\frac{\sqrt{5}-1}{2}}, 0)$, $\lambda \approx \pm 0.935i$, so these points are centers. A phase portrait for this situation is shown in Figure 4.

When $\alpha = -1$, $\beta = 1$ and $\gamma = -0.01$, there are equilibrium points at $(0, 0)$, $(\pm\sqrt{\frac{1+\sqrt{0.96}}{0.02}}, 0)$ and $(\pm\sqrt{\frac{1-\sqrt{0.96}}{0.02}}, 0)$. At $(0, 0)$, $\lambda = \pm i$, so this point is a center. At $(\pm\sqrt{\frac{1+\sqrt{0.96}}{0.02}}, 0)$, $\lambda = \pm i$, so these points are centers. At $(\pm\sqrt{\frac{1-\sqrt{0.96}}{0.02}}, 0)$, $\lambda = \pm 1.663$, so these points are saddles. A phase portrait for

this situation is shown in Figure 5.

3 Dynamics of the Unforced, Undamped Cubic-Quintic Duffing Oscillator

The unforced, undamped cubic-quintic Duffing oscillator is given by

$$x'' + \alpha x + \beta x^3 + \gamma x^5 = 0. \quad (11)$$

Varying the values of α , β and γ causes the behavior of the solution $x(t)$ to change, as depicted in bifurcation diagrams.¹ Equilibria can be either saddles or centers. The former are unstable points, whereas the latter are linearly stable. The qualitatively different situations that can occur are illustrated in the phase plots below.

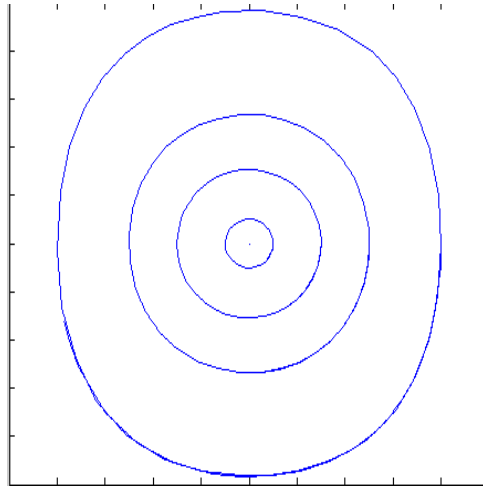


Figure 1: Phase plot with $\alpha = 1$, $\beta = 1$, and $\gamma = 1$.

The phase plot in Figure 1 shows the behavior of the oscillator when $\alpha = 1$, $\beta = 1$, and $\gamma = 1$. It is periodic with a center at $(0,0)$. This situation also occurs in the unforced cubic Duffing oscillator, as discussed previously.

The phase plot in Figure 2 shows the behavior of the oscillator when $\alpha = 1$, $\beta = -1$ and, $\gamma = -1$. Three equilibrium points are observed. There is a center at $(0, 0)$, and there are saddles at $(\pm 0.786, 0)$. As discussed above, this situation also occurs in the unforced cubic Duffing oscillator.

The phase plot in Figure 3 shows the behavior of the oscillator when $\alpha = 1$, $\beta = -1$, and $\gamma = 0.01$. Five equilibrium points are observed in the phase plot. There are centers at $(0, 0)$ and $(\pm 1.005, 0)$ and saddles at $(\pm 9.949, 0)$. This situation cannot occur in the cubic Duffing oscillator. The addition of the quintic term allows phase portraits with five equilibrium points to be generated.

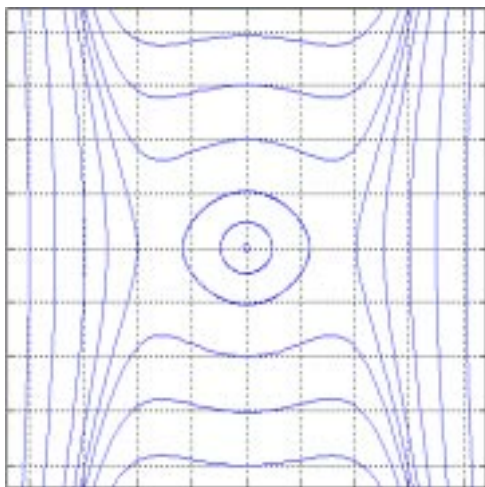


Figure 2: Phase plot with $\alpha = 1$, $\beta = -1$, and $\gamma = -1$.

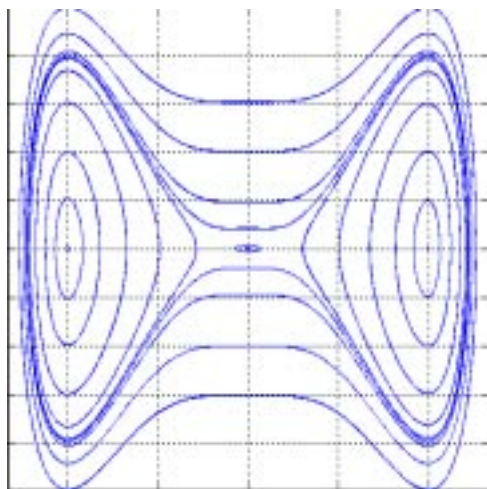


Figure 3: Phase plot with $\alpha = 1$, $\beta = -1$, and $\gamma = 0.01$.

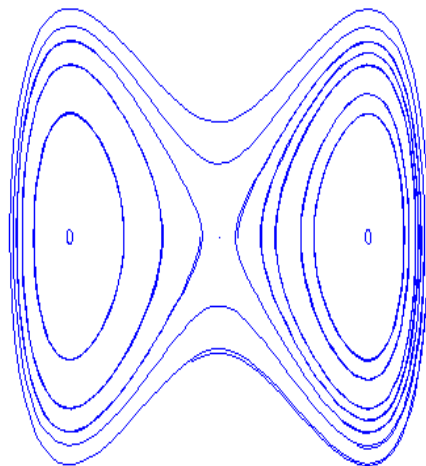


Figure 4: Phase portrait with $\alpha = -1$, $\beta = 1$, and $\gamma = 1$.

The phase portrait in Figure 4 shows the behavior of the oscillator when $\alpha = -1$, $\beta = 1$, and $\gamma = 1$. Three equilibrium points are observed. There are centers at $(\pm 0.786, 0)$ as well as a saddle at $(0, 0)$. This situation also occurs in the unforced cubic Duffing oscillator.

The phase portrait in Figure 5 shows the behavior of the oscillator when $\alpha = -1$, $\beta = 1$, and $\gamma = -0.01$. Five equilibrium points are observed in the phase plot. There are centers at $(\pm 1.01, 0)$ and saddles at $(0, 0)$ and $(\pm 9.949, 0)$. This situation cannot occur in the unforced cubic Duffing oscillator. As mentioned previously, the addition of the quintic term in the cubic-quintic Duffing oscillator allows phase plots with five equilibrium points to be generated.

As we have seen, phase portraits with one, three and five equilibrium points can be obtained with the cubic-quintic Duffing oscillator. There are also bifurcating points at which two or four equilibria can occur. For unforced cubic Duffing oscillators, phase plots with one and three equilibrium points can be generated. There are also bifurcating points at which two equilibria occur. Similarly, the addition of an x^7 term yields, with appropriate choices of parameters, phase portraits with seven equilibria. The Duffing oscillator can thereby be generalized to a class of dynamical systems by considering potentials $V(x)$ with increasingly many wells. The chaotic dynamics resulting from forcing such systems can also be analyzed.

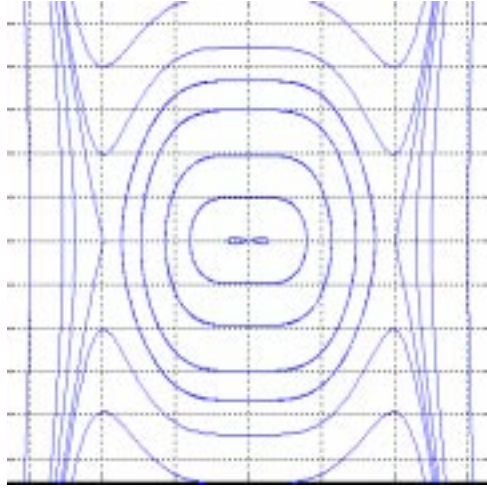


Figure 5: Phase portrait with $\alpha = -1$, $\beta = 1$, and $\gamma = -0.01$.

4 Dynamics of the Forced Cubic-Quintic Duffing Oscillator with a Single Sinusoidal Forcing Term

The driven, damped cubic-quintic Duffing oscillator with a single sinusoidal forcing is given by

$$x'' + \delta x' + \alpha x + \beta x^3 + \gamma x^5 = F \cos(\omega t). \quad (12)$$

One sets $\delta = 0$ in the absence of damping.

We compute phase portraits and Poincaré sections for various values of α , β , and γ . These are illustrated in the figures below. Fingerprints of the stable centers and the saddles that we observed in the unforced case can be seen in the phase plots of the forced cubic-quintic Duffing oscillator.

From (12), we obtain the non-autonomous dynamical system

$$\begin{aligned} x' &= y, \\ y' &= -\alpha x - \beta x^3 - \gamma x^5 + F \cos(\omega t), \end{aligned} \quad (13)$$

where we employ $F = 0.5$ and $\omega = 1$ in our simulations.

The phase portrait in Figure 6 is obtained when $\alpha = 1$, $\beta = 1$, and $\gamma = 1$. We observe fingerprints of the center from the unforced cubic-quintic Duffing oscillator.

Poincaré maps are used to investigate the flow near periodic orbits. Their dimensionality is one lower than that of the original dynamical system. Given an n -dimensional dynamical system,

$$x' = f(x), \quad x \in \mathbb{R}^n, \quad (14)$$

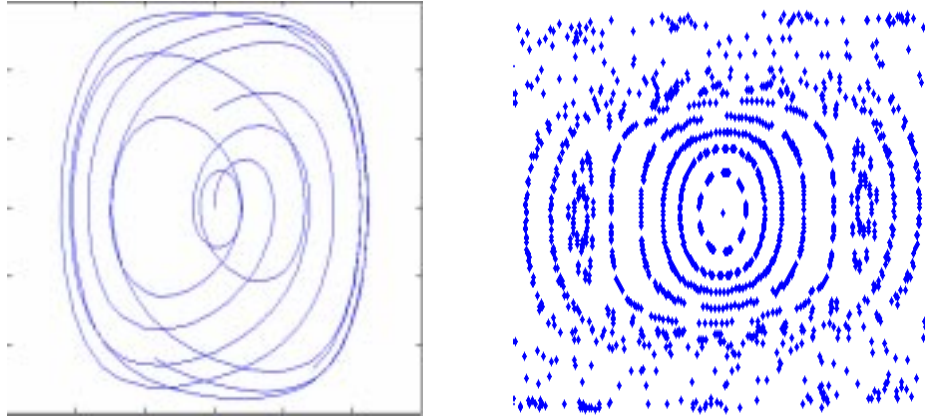


Figure 6: (a) Phase plot with $\alpha = 1$, $\beta = 1$, and $\gamma = 1$. (b) Poincaré map with $\alpha = 1$, $\beta = 1$, and $\gamma = 1$.

let S be an $n - 1$ dimensional surface of section that is transverse to the flow. A Poincaré map of (14) is a mapping of S to itself. They provide an extremely useful tool for studying chaotic dynamics.^{3,4,7,9} Closed orbits of the dynamical flow (14) are converted into fixed points of the Poincaré map. It is thus possible to demonstrate the existence of periodic solutions and examine their dynamics using Poincaré maps. In this paper, we construct Poincaré maps of forced Duffing oscillators by constructing surfaces of section corresponding to the period of the sinusoidal forcing.

The Poincaré map depicted in Figure 6 is obtained for the parameter values $\alpha = 1$, $\beta = 1$, and $\gamma = 1$. The left and right centers indicate the presence of a 2:1 resonance for this set of parameters. The one in the middle indicates the presence of a 1:1 resonance.

The phase portrait in Figure 7 is obtained for $\alpha = 1$, $\beta = -1$, and $\gamma = -1$. Fingerprints of the saddles from the unforced cubic-quintic Duffing oscillator are observed in the presence of forcing. The corresponding Poincaré map is also shown in Figure 7. The four outer centers demonstrate a 4:1 resonance. The one in the center indicates a 1:1 resonance. There is a saddle point between each pair of centers.

The phase portrait in Figure 8 is obtained when $\alpha = -1$, $\beta = 1$, and $\gamma = 1$. We observe fingerprints of the centers and saddle from the unforced case. The corresponding Poincaré map reveals several different resonances.

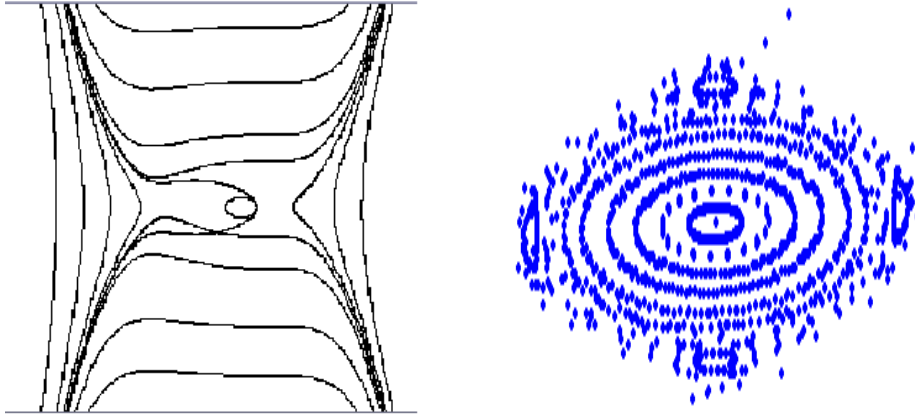


Figure 7: (a) Phase portrait with $\alpha = 1$, $\beta = -1$, and $\gamma = -1$. (b) Poincaré map with $\alpha = 1$, $\beta = -1$, and $\gamma = -1$.

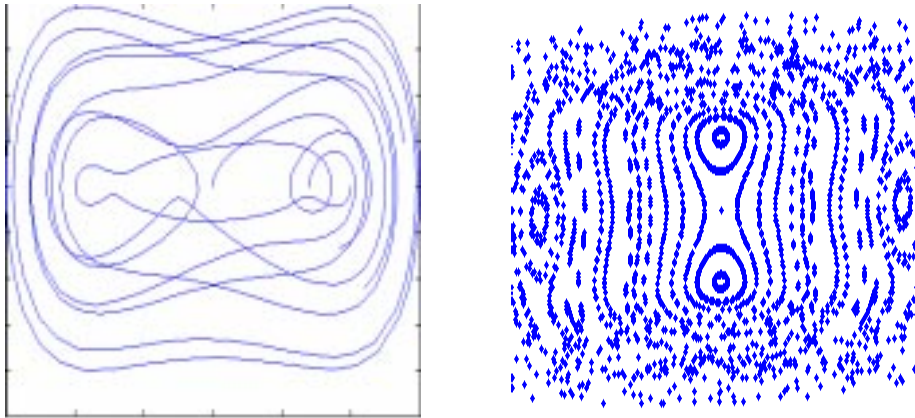


Figure 8: (a) Phase portrait with $\alpha = -1$, $\beta = 1$, and $\gamma = 1$. (b) Poincaré map with $\alpha = -1$, $\beta = 1$, and $\gamma = 1$.

5 Dynamics of the Cubic-Quintic Duffing Oscillator with Multiple-Frequency Sinusoidal Forcing

The forced, damped cubic-quintic Duffing oscillator with two sinusoidal forcing terms of different frequencies is described by

$$x'' + \delta x' + \alpha x + \beta x^3 + \gamma x^5 = F_1 \cos(\omega_1 t) + F_2 \cos(\omega_2 t). \quad (15)$$

Phase portraits of the multiple-frequency forced cubic-quintic Duffing oscillator for various values of α , β , and γ are illustrated below. When $\delta = 0$, equation (15) is undamped.

Increasing irregularity is observed with multiple-frequency forcing. The corresponding Poincaré maps should show (in principle) different regions of resonances due to the interaction of the two forcing terms. Chirikov's overlap criterion can be used to estimate the size and location of the resonance regions.⁷ However, the Poincaré maps we computed in this situation are similar to those we obtained for single-frequency sinusoidal forcing. We know from the theory⁷ that the more complex dynamical behavior discussed above is present, but we did not explore it numerically.

As a dynamical system, (15) is written

$$\begin{aligned} x' &= y, \\ y' &= -\alpha x - \beta x^3 - \gamma x^5 + F \cos(\omega_1 t) + F \cos(\omega_2 t), \end{aligned} \quad (16)$$

where $F := F_1 \equiv F_2 = 0.5$, $\omega_1 = 1$, and $\omega_2 = 4$ in our simulations. Note that different dynamical behavior is obtained depending on whether the forcing frequencies ω_1 , ω_2 are integer multiples, rational multiples, or irrational multiples of each other.³

The phase portrait in Figure 9 is obtained when $\alpha = 1$, $\beta = 1$, and $\gamma = 1$. We observe fingerprints of the center that occurs in the absence of forcing. The corresponding Poincaré map is also shown. The left and right centers indicate the presence of a 2:1 resonance for this set of parameters. The one in the middle indicate the presence of a 1:1 resonance.

For the set of parameters we examined, we observe more distortion in the phase portraits obtained with two sinusoidal forcing terms than in the phase portraits obtained with a single sinusoidal forcing term. The Poincaré sections we obtained for single-frequency and multiple-frequency forcing look similar.

The phase portrait in Figure 10 is obtained when $\alpha = 1$, $\beta = -1$, and $\gamma = -1$. We observe fingerprints of the unforced situation. The corresponding Poincaré map is also shown. One center is observed which indicates the presence of a 1:1 resonance.

More distortion is observed in the phase portraits obtained with two sinusoidal forcing terms than in the phase portraits obtained with a single sinusoidal forcing term for this set of parameters.

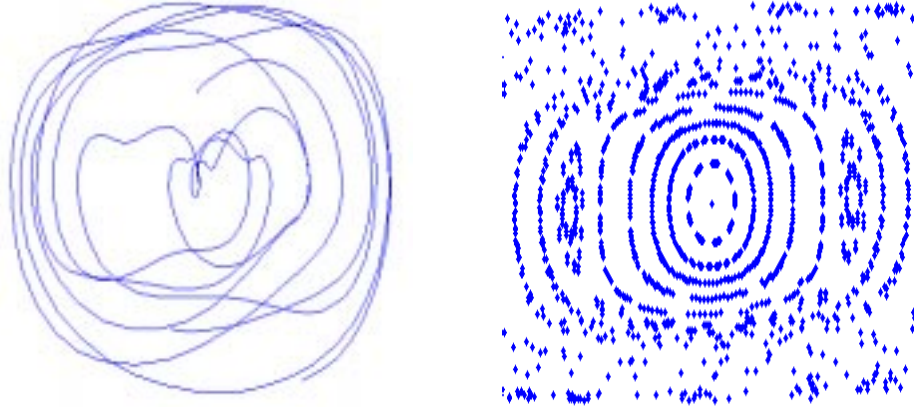


Figure 9: (a) Phase portrait with $\alpha = 1$, $\beta = 1$, and $\gamma = 1$. (b) Poincaré map with $\alpha = 1$, $\beta = 1$, $\gamma = 1$.

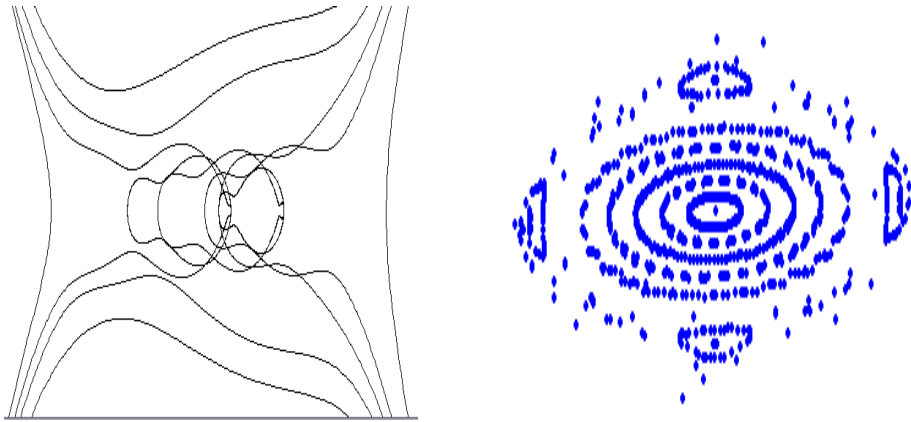


Figure 10: (a) Phase portrait with $\alpha = 1$, $\beta = -1$, and $\gamma = -1$. (b) Poincaré map with $\alpha = 1$, $\beta = -1$, and $\gamma = -1$.

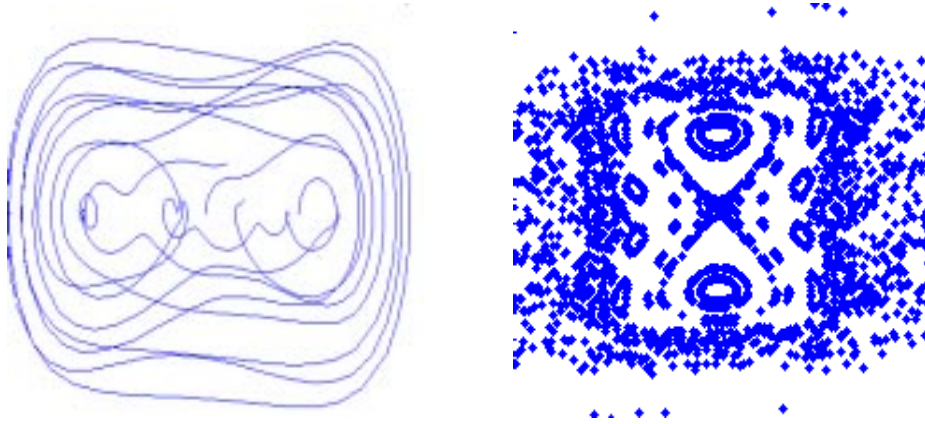


Figure 11: (a) Phase portrait with $\alpha = -1$, $\beta = 1$, and $\gamma = 1$. (b) Poincaré map with $\alpha = -1$, $\beta = 1$, $\gamma = 1$.

The phase portrait in Figure 11 is obtained when $\alpha = -1$, $\beta = 1$, and $\gamma = 1$. We observe fingerprints of the centers and saddle of the unforced case. The corresponding Poincaré map reveals several different resonances.

6 Perturbative Analysis

The method of averaging is a powerful perturbation method in which solutions of autonomous dynamical systems can be used to approximate solutions of complicated time-varying dynamical systems.^{7,8} In particular, it can be used to show that periodic motions exist and to approximate them for small non-autonomous perturbations.

Consider the forced cubic-quintic Duffing oscillator with a single sinusoidal forcing term, given by

$$x'' + \delta x' + \alpha x + \varepsilon \beta x^3 + \varepsilon \gamma x^5 = \varepsilon A \cos(t + \psi(t)) \quad (17)$$

When $\delta = 0$, (17) is undamped. When $\varepsilon = 0$, solutions to equation (17) have the following form

$$\begin{aligned} x &= a \cos(t + \psi), \\ x' &= -a \sin(t + \psi). \end{aligned} \quad (18)$$

where a and ψ are constants.

When ε is small, solutions to equation (17) are similar to (18), except that a and ψ are now slowly-varying functions of time:

$$\begin{aligned} x &= a(t) \cos(t + \psi(t)), \\ x' &= -a(t) \sin(t + \psi(t)). \end{aligned} \quad (19)$$

Additionally,

$$x'' = -a'(t) \sin(t + \psi(t)) - a(t)\psi'(t) \cos(t + \psi(t)). \quad (20)$$

Substituting equations (19) and (20) into (17) and solving for a' and ψ' yields

$$\begin{aligned} a' &= -a(1 - \alpha) \sin(t + \psi(t)) \cos(t + \psi(t)) + \varepsilon\beta a^3 \cos^3(t + \psi(t)) \sin(t + \psi(t)) \\ &\quad + \varepsilon\gamma a^5 \cos^5(t + \psi(t)) \sin(t + \psi(t)) - \varepsilon A \cos(t + \psi(t)) \sin(t + \psi(t)), \\ \psi' &= \sin^2(t + \psi(t)) + \alpha \cos^2(t + \psi(t)) + \varepsilon\beta a^2 \cos^4(t + \psi(t)) \\ &\quad + \varepsilon\gamma a^4 \cos^6(t + \psi(t)) - \frac{\varepsilon A}{a} \cos^2(t + \psi(t)). \end{aligned} \quad (21)$$

One now introduces an approximation in the form of a near-identity transformation written as a power series in ε :

$$\begin{aligned} a &= \bar{a} + \varepsilon\omega_1(\bar{a}, \bar{\psi}) + O(\varepsilon^2), \\ \psi &= \bar{\psi} + \varepsilon\omega_2(\bar{a}, \bar{\psi}) + O(\varepsilon^2) \end{aligned} \quad (22)$$

where ω_1 and ω_2 are generating functions, chosen to make \bar{a} and $\bar{\psi}$ as simple as possible.

Substituting (21) into equation (22) and solving for \bar{a}' , ψ gives

$$\begin{aligned} \bar{a}' &= a' - \varepsilon\omega_1' + O(\varepsilon^2) \\ &= -a(1 - \alpha) \sin(t + \psi(t)) \cos(t + \psi(t)) + \varepsilon\beta a^3 \cos^3(t + \psi(t)) \sin(t + \psi(t)) \\ &\quad + \varepsilon\gamma a^5 \cos^5(t + \psi(t)) \sin(t + \psi(t)) - \varepsilon A \cos(t + \psi(t)) \sin(t + \psi(t)) - \varepsilon\omega_1' + O(\varepsilon^2), \end{aligned} \quad (23)$$

where ω_1 is chosen to remove all ψ -dependent terms and ω_1' denotes its time derivative.

Additionally,

$$\begin{aligned} \bar{a}' &= O(\varepsilon^2), \\ \bar{a} &= c_1. \end{aligned} \quad (24)$$

Substituting (21) into equation (22) and solving for ψ' yields

$$\begin{aligned} \psi' &= \psi(t) - \varepsilon\omega_2' + O(\varepsilon^2) \\ &= \sin^2(t + \psi(t)) + \alpha \cos^2(t + \psi(t)) + \varepsilon\beta a^2 \cos^4(t + \psi(t)) + \varepsilon\gamma a^4 \cos^6(t + \psi(t)) \\ &\quad - \frac{\varepsilon A}{a} \cos^2(t + \psi(t)) - \varepsilon\omega_2' + O(\varepsilon^2). \end{aligned} \quad (25)$$

Removing higher-order terms of ε gives

$$\begin{aligned} \psi' &= \frac{1 + \alpha}{2} + \frac{3}{8}\varepsilon\beta a^2 - \frac{5}{16}\varepsilon\gamma a^4 - \varepsilon\frac{A}{2a} + O(\varepsilon^2), \\ \psi &= \left[\frac{1 + \alpha}{2} + \frac{3}{8}\varepsilon\beta a^2 - \frac{5}{16}\varepsilon\gamma a^4 - \frac{\varepsilon A}{2a} + O(\varepsilon^2) \right] t + c_2. \end{aligned} \quad (26)$$

One now substitutes equations (24) and (310) into (19) to obtain an approximate solution for x :

$$\begin{aligned} x &= a \cos(t + \psi(t)) = [\bar{a} + O(\varepsilon)] \cos[t + \psi(t) + O(\varepsilon)] \\ &= c_1 \cos \left(\left[\frac{1 + \alpha}{2} + \frac{3}{8} \varepsilon \beta a^2 - \frac{5}{16} \varepsilon \gamma a^4 - \frac{\varepsilon A}{2a} + O(\varepsilon^2) \right] t + c_2 \right) + O(\varepsilon). \end{aligned} \quad (27)$$

For $\alpha = 1$, $\beta = 1$, $\gamma = 1$, one obtains

$$x = c_1 \cos \left(\left[1 + \frac{3}{8} \varepsilon a^2 - \frac{5}{16} \varepsilon a^4 - \frac{\varepsilon A}{2a} + O(\varepsilon^2) \right] t + c_2 \right) + O(\varepsilon^2). \quad (28)$$

For $\alpha = 1$, $\beta = -1$, $\gamma = -1$, one obtains

$$x = c_1 \cos \left(\left[\frac{3}{8} \varepsilon \beta a^2 + \frac{5}{16} \varepsilon a^4 - \frac{\varepsilon A}{2a} + O(\varepsilon^2) \right] t + c_2 \right) + O(\varepsilon^2). \quad (29)$$

For $\alpha = -1$, $\beta = 1$, $\gamma = 1$, one obtains

$$x = c_1 \cos \left(\left[\frac{3}{8} \varepsilon \beta a^2 - \frac{5}{16} \varepsilon \gamma a^4 - \frac{\varepsilon A}{2a} + O(\varepsilon^2) \right] t + c_2 \right) + O(\varepsilon^2). \quad (30)$$

The near-identity transformation used in the averaging method has two advantages. First, after solving for \bar{a} and $\bar{\psi}$, a higher degree of accuracy for the solution is obtained by transforming back to a and ψ . Second, by using the near-identity transformation, the averaging procedure can be extended to higher orders of approximation by iterating the process.⁷

The approximate solution of the cubic-quintic Duffing oscillator for each situation is obtained by substituting the different parameters into the general form (27). One obtains similar approximate solutions obtained using the method of averaging and Lindstedt method's, which is a singular perturbation (multiple scale) method in which time is stretched to incorporate period-amplitude relationships into an approximate solution that behaves periodically.^{7,8} Because it is nonlinear, the period of oscillations in the cubic-quintic Duffing equation depends on their amplitude. Hence, one can also employ Lindstedt's method to study its periodic solutions.

In this formulation, the forced cubic-quintic Duffing oscillator with a single sinusoidal forcing term is given by

$$x'' + \delta x' + \alpha x + \beta \varepsilon x^3 + \gamma \varepsilon x^5 = \varepsilon A \cos(\omega t). \quad (31)$$

When $\delta = 0$, (31) is undamped. One stretches time by defining

$$\tau := \omega t, \quad (32)$$

where the stretching frequency is

$$\omega = 1 + k_1 \varepsilon + k_2 \varepsilon^2 + \dots \quad (33)$$

Expanding x in a power series in ε yields

$$x(\varepsilon) = x_0(\tau) + \varepsilon x_1(\tau) + \varepsilon^2 x_2(\tau) + \dots \quad (34)$$

Substituting (33) into (34) gives

$$\omega^2 x'' + \alpha x + \beta \varepsilon x^3 + \gamma \varepsilon x^5 = \varepsilon A \cos \tau. \quad (35)$$

Substituting (34) into (35) and collecting terms of like powers in the perturbation parameter ε yields the following equations:

$$\begin{aligned} \varepsilon^0 : x_0'' + \alpha x_0 &= 0, \\ \varepsilon^1 : x_1'' + \alpha x_1 + \beta \varepsilon x_0^3 + \gamma \varepsilon x_0^5 &= \varepsilon A \cos \tau. \end{aligned} \quad (36)$$

At leading order, one obtains

$$x_0 = a \cos \tau, \quad (37)$$

which is substituted into equation (36). Removing secular terms yields the condition

$$k_1 = \frac{3}{8}\beta a^2 + \frac{5}{16}\gamma a^4 - \frac{A}{2a} \quad (38)$$

and hence the frequency-amplitude relation

$$\omega = 1 + k_1 \varepsilon + O(\varepsilon^2) = 1 + \left(\frac{3}{8}\beta a^2 + \frac{5}{16}\gamma a^4 - \frac{A}{2a} \right) \varepsilon + O(\varepsilon^2). \quad (39)$$

One obtains the period-amplitude relation with the expression $T = 2\pi/\omega$. The leading-order approximate solution is then

$$x_0 = a \cos \left(\left[1 + \left(\frac{3}{8}\beta a^2 + \frac{5}{16}\gamma a^4 - \frac{A}{2a} \right) \varepsilon \right] t \right). \quad (40)$$

We then substitute (40) into (36) to obtain an approximation for x_1 :

$$x_1 = \frac{4\beta a^3 + 5\gamma a^5}{16(9 - \alpha)} \cos 3\tau - \frac{\gamma a^5}{16(\alpha - 25)} \cos 5\tau. \quad (41)$$

Therefore,

$$x = a \cos \left(\left[1 + \left(\frac{3}{8}\beta a^2 + \frac{5}{16}\gamma a^4 - \frac{A}{2a} \right) \varepsilon \right] t \right) + \varepsilon \left[\frac{4\beta a^3 + 5\gamma a^5}{16(9 - \alpha)} \cos 3\tau - \frac{\gamma a^5}{16(\alpha - 25)} \cos 5\tau \right] + O(\varepsilon^2). \quad (42)$$

One can then substitute x_0 and x_1 into the $O(\varepsilon^2)$ equation to obtain k_2 . This process can be continued indefinitely to obtain as close an estimate to x as one wishes (for small ε). We now consider a few specific values of α , β , and γ .

When $\alpha = 1$, $\beta = 1$, and $\gamma = 1$,

$$\begin{aligned}\omega &= 1 + \left(\frac{3}{8}a^2 + \frac{5}{16}a^4 - \frac{A}{2a} \right) \varepsilon + O(\varepsilon^2), \\ x &= a \cos \left(\left[1 + \left(\frac{3}{8}a^2 + \frac{5}{16}a^4 - \frac{A}{2a} \right) \varepsilon \right] t \right) + \varepsilon \left[\left(\frac{5}{128}a^5 + \frac{1}{32}a^3 \right) \cos 3\tau + \frac{9}{384} \cos 5\tau \right] + O(\varepsilon^2).\end{aligned}\tag{43}$$

When $\alpha = 1$, $\beta = -1$, and $\gamma = -1$,

$$\begin{aligned}\omega &= 1 + \left(-\frac{3}{8}a^2 - \frac{5}{16}a^4 - \frac{A}{2a} \right) \varepsilon + O(\varepsilon^2), \\ x &= a \cos \left(\left[1 + \left(-\frac{3}{8}a^2 - \frac{5}{16}a^4 - \frac{A}{2a} \right) \varepsilon \right] t \right) + \varepsilon \left[\left(-\frac{5}{128}a^5 - \frac{1}{32}a^3 \right) \cos 3\tau - \frac{1}{384}a^5 \cos 5\tau \right] + O(\varepsilon^2).\end{aligned}\tag{44}$$

When $\alpha = -1$, $\beta = 1$, and $\gamma = 1$,

$$\begin{aligned}\omega &= 1 + \left(\frac{3}{8}a^2 + \frac{5}{16}a^4 - \frac{A}{2a} \right) \varepsilon + O(\varepsilon^2), \\ x &= a \cos \left(\left[1 + \left(\frac{3}{8}a^2 + \frac{5}{16}a^4 - \frac{A}{2a} \right) \varepsilon \right] t \right), \\ +\varepsilon &\left[\left(\frac{1}{32}a^5 + \frac{1}{40}a^3 \right) \cos 3\tau + \frac{1}{416}a^5 \cos 5\tau \right] + O(\varepsilon^2).\end{aligned}\tag{45}$$

7 Conclusions

In this paper, we investigated forced cubic-quintic Duffing oscillators using both numerical and analytical techniques. We considered the unforced, undamped cubic-quintic Duffing oscillator, the forced cubic-quintic Duffing oscillator with a single sinusoidal forcing term, and the forced cubic-quintic Duffing oscillator with two sinusoidal forcing terms of multiple frequencies.

The dynamical behavior of the forced cubic-quintic Duffing oscillator, which depends on the parameter values one considers, can be studied numerically using phase portraits and Poincaré sections. Situations with one, three and five equilibrium points can be obtained from the unforced, undamped cubic-quintic Duffing oscillator by varying the system parameters.

Phase portraits and Poincaré sections also allow one to compare the effects of single-frequency and dual-frequency sinusoidal forcing with unforced (integral) situations. With Poincaré sections, we also observed the onset of resonances.

We also employed perturbation methods such as Lindstedt's method and the method of averaging to investigate periodic orbits of cubic-quintic Duffing oscillators analytically.

In sum, my efforts to investigate the cubic-quintic Duffing oscillator with numerical and analytical methods have yielded fairly successful results. Attempts

to extend the methods that were used in analyzing cubic Duffing oscillators to cubic-quintic Duffing oscillators have highlighted several special characteristics of the latter system. In particular, situations with five equilibrium points can only be observed in the cubic-quintic Duffing oscillator because of the presence of the additional quintic term. The numerical simulations will be helpful in analyzing the dynamics of the system when investigating the cubic-quintic Duffing oscillator analytically in future. In particular, although we observed the onset of resonance bands, we did not analyze them. In addition to refined numerics, approaches such as Chirikov's overlap criterion can be used to study their global dynamical consequences in detail.

Acknowledgements

I am extremely grateful to Professor Mason Porter of the School of Mathematics at Georgia Tech for his help in simulating the plots, explaining many of the complex mathematical theories as well as revising the paper.

References

- [1] Vincent T. Coppola. *Averaging of Strongly Nonlinear Oscillators Using Elliptic Functions*. PhD thesis, Cornell University, August 1989.
- [2] Herbert Goldstein. *Classical Mechanics*. Addison-Wesley Publishing Company, Reading, MA, 2nd edition, 1980.
- [3] John Guckenheimer and Philip Holmes. *Nonlinear Oscillations, Dynamical Systems, and Bifurcations of Vector Fields*. Number 42 in Applied Mathematical Sciences. Springer-Verlag, New York, NY, 1983.
- [4] Allan J. Lichtenberg and M. A. Leiberman. *Regular and Chaotic Dynamics*. Number 38 in Applied Mathematical Sciences. Springer-Verlag, New York, NY, 2nd edition, 1992.
- [5] Mason A. Porter and Predrag Cvitanović. Modulated amplitude waves in Bose-Einstein condensates. ArXiv: nlin.CD/0307032, Submitted, July 2003.
- [6] Mason A. Porter and Predrag Cvitanović. A perturbative analysis of modulated amplitude waves in Bose-Einstein condensates. ArXiv: nlin.CD/0308024, Submitted, August 2003.
- [7] Richard H. Rand. *Topics in Nonlinear Dynamics with Computer Algebra*, volume 1 of *Computation in Education: Mathematics, Science and Engineering*. Gordon and Breach Science Publishers, USA, 1994.
- [8] Richard H. Rand. Lecture notes on nonlinear vibrations. a free online book available at <http://www.tam.cornell.edu/randdocs/nlvibe45.pdf>, 2003.

- [9] Steven H. Strogatz. *Nonlinear Dynamics and Chaos*. Addison-Wesley, Reading, MA, 1994.